

Reaction between CH₃ and H₂ at Combustion Temperatures

Hyun Ju Baeck, Kuan Soo Shin*, H. Yang[†], V. Lissianski[†], and W. C. Gardiner, Jr.[†]

Department of Chemistry, Soong Sil University, Seoul 156-743, Korea

[†]Department of Chemistry and Biochemistry,

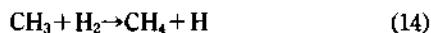
The University of Texas at Austin, Austin, Texas 78712, U.S.A.

Received March 14, 1995

The reaction between CH₃ radicals and H₂ was investigated behind incident shock waves at temperatures between 1308 and 1825 K by following the consumption of CH₃ using a time resolved UV absorption method at 213.9 nm. The rate coefficient expression $1.10 \times 10^{13} \exp(-7370 \text{ K}/T) \text{ cm}^3 \text{ mol}^{-1} \text{ s}^{-1}$ for the reaction of CH₃ with H₂ was derived.

Introduction

The reaction between CH₃ with H₂,



and its reverse reaction play important roles in methane pyrolysis and combustion. Numerous experimental¹⁻⁶ and theoretical⁷⁻¹⁰ studies of reaction 14 (see Table 2) and its reverse reaction have been reported, and extensive review articles¹¹⁻¹⁴ have been published. Nearly all of the previous investigations of CH₃ with H₂ and its reverse reaction have been measured by indirect methods. Möller *et al.*⁵ measured $k_{14}(T)$ more directly in a shock tube over the temperature range from 1066 to 2166 K utilizing the UV absorption of CH₃ at 216.5 nm in the pyrolysis of azomethane or tetramethyltin to generate methyl radical. Their data were fit to the Arrhenius expression $k_{14}(T) = 2.0 \times 10^{13} \exp(-7200 \text{ K}/T) \text{ cm}^3 \text{ mol}^{-1} \text{ s}^{-1}$. Rabinowitz *et al.*⁶ also directly measured the rate of the reverse reaction, CH₄ + H → CH₃ + H₂, using a flash photolysis-shock tube technique in the temperature range from 897 to 1729 K. They reported $k_{14}(T) = 3.1 \times 10^{12} \exp(-5940 \text{ K}/T)$ and $k_{-14}(T) = 1.1 \times 10^{14} \exp(-6440 \text{ K}/T) \text{ cm}^3 \text{ mol}^{-1} \text{ s}^{-1}$. The agreement of those recent two results is not good. The Möller *et al.*⁵ expression is about 100% larger than the Rabinowitz *et al.*⁶ expression at 1200 K and more than 150% larger at 1700 K. The purpose of the present investigation is to measure the rate coefficient of the CH₃ reaction with H₂ at combustion temperatures using spectroscopic determination of CH₃ concentration profiles during the thermal decomposition of azomethane or methyl iodide in the presence of large excess of H₂.

Experiment

The experiments were done utilizing incident shock waves in a Monel shock tube of 7.62 cm inside diameter which was described in detail elsewhere¹⁵. Shock parameters were computed from measured incident shock velocities by standard methods¹⁶ using JANAF¹⁷ and NASA¹⁸ thermochemical data under the assumption of steady flow and no wall boundary layer formation. The concentration of CH₃ radicals was measured using the absorption of 213.9 nm light from a Pen-Ray Zn arc lamp (Ultra-Violet Products) directed through two opposed sapphire windows combined with two slits

(width 1 mm) and an interference filter of 9 mm (fwhm) band-pass and 19% peak transmission onto an EMI 9526B photomultiplier tube. The signal-to-noise ratio of the transmitted beam was about 50, resulting in a detection limit of about 200 mol/m³ for CH₃. The transmitted light intensity was recorded with a Nicolet Explorer II storage oscilloscope and stored on floppy disks for later use. Azomethane, synthesized according to the method of Renaud and Leitch,¹⁹ and methyl iodide (99.5%, Aldrich) were used as sources of CH₃ radicals. Ar (99.999%, Matheson) and H₂ (99.97%, Matheson) were used without further purification. Test gas mixtures were prepared manometrically and allowed to stand for 48 hours before use.

Results and Discussion

The removal of CH₃ by H₂ was investigated behind incident shock waves at temperatures between 1308 and 1825 K and densities from 2.6 to 5.9 mol/m³. The mixture compositions studied are shown in Table 1. The concentrations of azomethane and methyl iodide were limited to 3000 ppm to suppress the contribution of CH₃ self-reactions and the influence of their reaction products. High H₂ concentrations were selected to enhance the rate of the CH₃ + H₂ reaction.

A typical absorption profile at 213.9 nm is shown in Figure 1. The steep rise in absorption due to production of CH₃ by thermal decomposition of azomethane or methyl iodide is followed by decay due to the reaction of CH₃ with H₂ and the CH₃ self-reactions. The absorption at long times is due to eventual accumulation of products of reaction. Even though the contributions of other species which make absorption at this wavelength were small, they were also included

Table 1. Mixture Compositions in Ar

	(CH ₃) ₂ N ₂ (%)	H ₂ (%)	T (K)	ρ (mol/m ³)
1	0.0994	5.32	1308-1825	2.8-5.9
2	0.0986	10.2	1323-1693	2.7-5.3
	CH ₃ I (%)	H ₂ (%)	T (K)	ρ (mol/m ³)
3	0.202	5.31	1439-1793	2.6-5.1
4	0.302	10.0	1498-1671	2.8-3.7

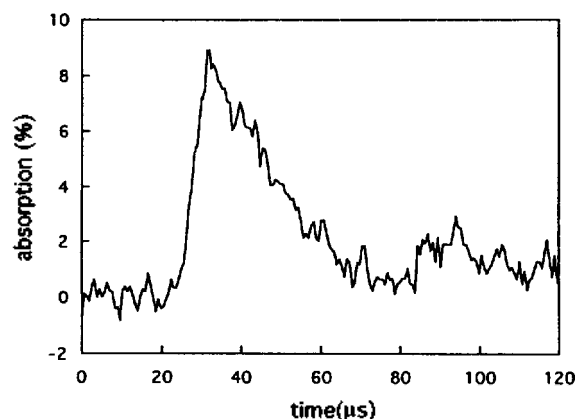


Figure 1. Typical experimental absorption profile of CH_3 at 213.9 nm. Shock conditions: 0.0994% $\text{C}_2\text{H}_6\text{N}_2$, 5.32% H_2 in Ar, $T_2=1308$ K, $\rho_2=5.63$ mol/m³.

Table 2. Reaction mechanism

Elementary reaction	log A	n	Ea (KJ)
1a $\text{C}_2\text{H}_6\text{N}_2 = \text{CH}_3 + \text{CH}_3 + \text{N}_2$	9.08	-	98.9
1b $\text{CH}_3\text{I} = \text{CH}_3 + \text{I}$	14.48	-	133.9
2 $\text{C}_2\text{H}_6 = \text{CH}_3 + \text{CH}_3$	58.26	-10.61	412.4
Falloff parameters: 1.060×10^{26} , -2.792, 389.6, 0.310, 518, 445			
3 $\text{CH}_3 + \text{CH}_3 = \text{C}_2\text{H}_6 + \text{H}$	12.45	-	40.0
4 $\text{CH}_3 + \text{CH}_3 = \text{C}_2\text{H}_4 + \text{H}_2$	12.78	-	69.0
5 $\text{CH}_3 + \text{C}_2\text{H}_6 = \text{CH}_4 + \text{C}_2\text{H}_5$	-0.05	4.00	40.5
6 $\text{CH}_3 + \text{C}_2\text{H}_4 = \text{CH}_4 + \text{C}_2\text{H}_3$	11.62	11.62	46.4
7 $\text{CH}_3 + \text{C}_2\text{H}_2 = \text{CH}_4 + \text{C}_2\text{H}$	-3.36	5.00	34.7
8 $\text{C}_2\text{H}_6 + \text{H} = \text{C}_2\text{H}_5 + \text{H}_2$	14.12	-	39.0
9 $\text{C}_2\text{H}_5 = \text{C}_2\text{H}_4 + \text{H}$	40.67	-7.04	182.0
Falloff parameters: 4.97×10^{10} , 0.732, 154.2, 0.278, 1.032×10^6 , 754.2			
10 $\text{C}_2\text{H}_5 + \text{H} = \text{C}_2\text{H}_4 + \text{H}_2$	12.23	-	0.0
11 $\text{CH}_3 + \text{M} = \text{CH}_2 + \text{H} + \text{M}$	16.00	-	377.0
12 $\text{CH}_2 + \text{CH}_3 = \text{C}_2\text{H}_4 + \text{H}$	13.30	-	0.0
13 $\text{CH}_4 = \text{CH}_3 + \text{H}$	36.80	-5.25	451.3
Falloff parameters: 3.71×10^{17} , -0.558, 438.8, 0.483, 409.3, 341.3			
14 $\text{CH}_3 + \text{H}_2 = \text{CH}_4 + \text{H}$	12.76	-	53.0
15 $\text{C}_2\text{H}_4 + \text{M} = \text{C}_2\text{H}_2 + \text{H}_2 + \text{M}$	17.41	-	332.0
16 $\text{C}_2\text{H}_4 + \text{M} = \text{C}_2\text{H}_3 + \text{H} + \text{M}$	17.41	-	404.0
17 $\text{H} + \text{C}_2\text{H}_4 = \text{H}_2 + \text{C}_2\text{H}_3$	11.50	0.70	33.5
18 $\text{CH}_3 + \text{C}_2\text{H}_2 = \text{C}_2\text{H}_4 + \text{CH}_2$	-3.36	5.00	34.7
19 $\text{C}_2\text{H}_3 + \text{M} = \text{C}_2\text{H}_2 + \text{H} + \text{M}$	39.08	-7.17	212.0
20 $\text{C}_2\text{H}_3 + \text{H} = \text{C}_2\text{H}_2 + \text{H}_2$	13.30	-	0.0
21 $\text{H}_2 + \text{M} = \text{H} + \text{H} + \text{M}$	12.35	0.50	387.0
22 $\text{CH}_3 + \text{CH}_3 = \text{CH}_4 + \text{CH}_2$	9.23	0.56	52.6

Notes: Units are cm³, mol, s and kJ. The rate coefficients for **1a** and **1b** were taken from Möller *et al.*⁵ and Davidson *et al.*²² respectively. For reactions 2, 9 and 13 the tabulated parameters refer to the low pressure limit rate coefficients; the first three of the falloff parameters listed for these reactions are log A, n and Ea for their high pressure limit rate coefficients, and the remaining falloff parameters are the a, b and c values that define the temperature dependence of the broadening factor.

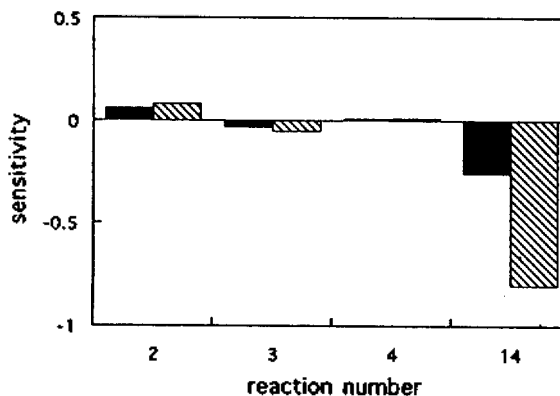


Figure 2. Logarithmic response sensitivity spectra²³ for the effective rate coefficient (k_{eff}) for 0.0994% $\text{C}_2\text{H}_6\text{N}_2$, 5.32% H_2 in Ar, $T_2=1560$ K, $P_1=24.6$ Torr. The filled and striped bars were computed by multiplying and dividing the Table 2 rate coefficient value by 1.5. Sensitivities less than 0.01 are not shown.

in the computer simulations described below using the extinction coefficients measured by Gardiner *et al.*²⁰ under similar conditions.

The reaction mechanism used to analyze the experimental data is shown in Table 2. It was constructed starting with the Hwang *et al.*²¹ mechanism used to determine the rate coefficients for CH_3 self-reactions. These rate coefficient expressions had been optimized to describe CH_3 concentration profiles in azomethane argon mixtures shock heated in the same apparatus to conditions (temperatures from 1300 to 1700 K, densities from 2 to 9 mol/m³) that were similar to ours. The rate coefficient expressions for $\text{C}_2\text{H}_6\text{N}_2$ and CH_3I decompositions were taken from Möller *et al.*⁵ and Davidson *et al.*²² respectively. In the final data analysis, literature values of all rate coefficient parameters were used without modification except for those of reaction 14. Sensitivity calculations²³ (Fig. 2) showed that reaction 14 and CH_3 self-reactions contribute substantially to the CH_3 decay profiles.

For conditions where reaction 14 removes the main part of the CH_3 radicals and the decomposition of azomethane is fast, the decrease of the CH_3 concentration should come close to following first-order kinetics, *i.e.*,

$$d[\text{CH}_3]/dt = -k_{\text{eff}} [\text{CH}_3]$$

where $k_{\text{eff}} = k_{14} [\text{H}_2] + k_{\text{self}} [\text{CH}_3]$. For small contributions of CH_3 self-reactions

$$\ln ([\text{CH}_3]_0/[\text{CH}_3]) = k_{\text{eff}} t \quad (1)$$

The absorption at 213.9 nm is almost entirely due to CH_3

$$\log(I_0/I) = \epsilon_{\text{CH}_3} [\text{CH}_3] d$$

where d is the absorption path length and I is the transmitted intensity. Thus, the CH_3 concentration is related to the transmitted intensity by

$$[\text{CH}_3] = \log(I_0/I) / (\epsilon_{\text{CH}_3} d)$$

$$[\text{CH}_3]_0 = \log(I_0/I_{\text{max}}) / (\epsilon_{\text{CH}_3} d)$$

The decrease of CH_3 follows

$$[\text{CH}_3]_0/[\text{CH}_3] = \log(I_0/I_{\text{max}}) / \log(I_0/I) \quad (2)$$

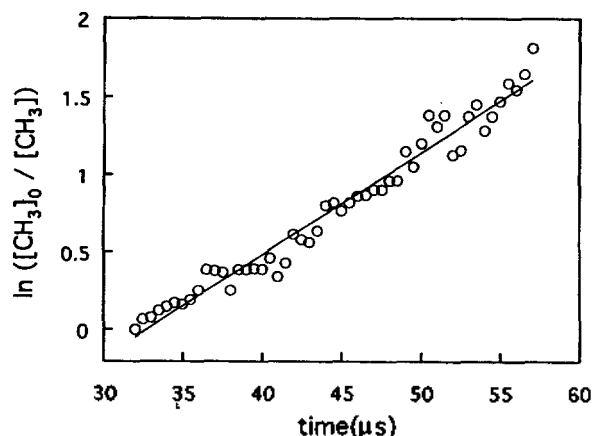


Figure 3. Pseudo-first-order plot of CH₃ concentration for the experiment in Figure 1. See Eq. 2 and the discussion in the text.

where I_{max} is the transmitted intensity at maximum absorption in an experiment. From Eqs. (1) and (2) the effective rate coefficient k_{eff} of CH₃ disappearance is given by

$$k_{eff} = (d/dt) [\ln \{ \log(I_0/I_{max}) / \log(I_0/I) \}] \quad (3)$$

This analysis, based on the assumption of instantaneous azomethane decomposition and first-order decay, thus suggests that the right-hand side (rhs) of Eq. 3 should be a suitable measure of the reaction rate for the CH₃ loss, even though the actual removal mechanism is known to be complicated.

Figure 3 shows a plot of the rhs of Eq. 2 as a function of time under the conditions of the experiment shown in Figure 1. It shows that the intensity profile follows a first-order rate law closely for the main part of the observed disappearance of CH₃. For small contributions of CH₃ self-reactions the value of k_{eff} does not depend on the extinction coefficient of CH₃ at all, and k_{eff} can therefore be used in general for comparisons between experimental and calculated absorption profiles with confidence that the rate coefficient influences can be isolated from the value of the CH₃ extinction coefficient. As shown later, it also permits an evaluation of the extinction coefficient of CH₃ from measurements of I_{max} . Experimental results were compared with calculations taking into account the self-reactions of CH₃ and the finite rate of azomethane decomposition as follows. The CH₃ absorption profiles were simulated for the conditions of each run with the help of the mechanism in Table 2 using a predecessor of the LSODE²⁴ program for the integration of the differential equations, and the value of k_{14} was adjusted until the experimental and calculated values of k_{eff} coincided. The results of k_{14} calculations done in this manner are presented in Figure 4 together with the results of Möller *et al.*,⁵ Rabinowitz *et al.*,⁶ Clark and Dove,⁷ Schatz *et al.*,⁸ and Joseph *et al.*¹⁰ A linear least-squares fit to the data results in the expression

$$k_{14} = 1.10 \times 10^{13} \exp(-7370 \text{ K}/T) \text{ cm}^3 \text{ mol}^{-1} \text{ s}^{-1}$$

for the temperature range from 1308 to 1825 K. The present result is in better agreement with the expression of Rabinowitz *et al.*⁶ than that of Möller *et al.*⁵ The values of Schatz

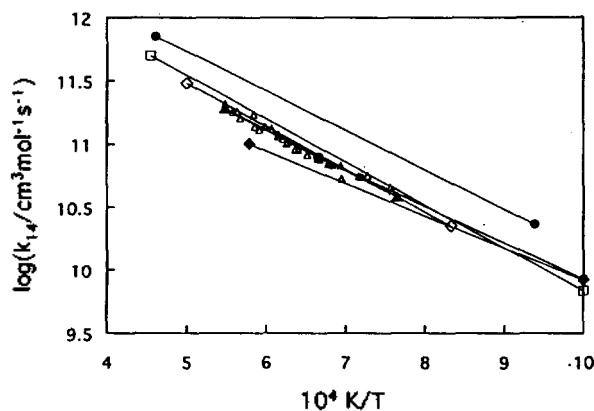


Figure 4. Dependence of k_{14} on temperature: open triangles represent our experimental results, and solid triangle line is a least-square fit of them; filled circle line, Möller *et al.*⁵; filled diamond line, Rabinowitz *et al.*⁶; open diamond line, Clark and Dove⁷; open square line, Schatz *et al.*⁸; open circle line, Joseph *et al.*¹⁰

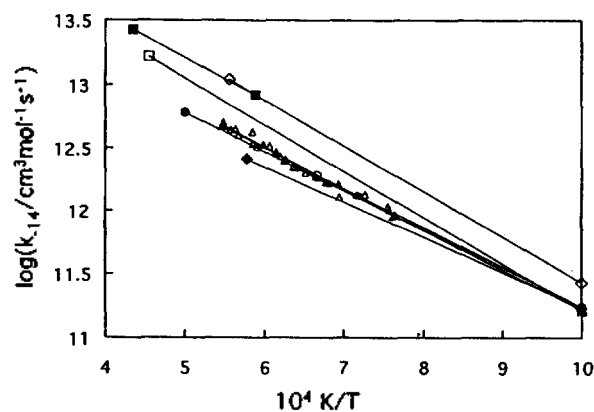


Figure 5. Dependence of k_{-14} on temperature: open triangles represent our experimental results, and solid triangle line is a least-square fit of them; filled square line, Roth and Just⁴; filled diamond line, Rabinowitz *et al.*⁶; open diamond line, Clark and Dove⁷; open square line, Schatz *et al.*⁸; open circle line, Joseph *et al.*¹⁰; filled circle line, Allara and Shaw¹³.

*et al.*⁸ and Clark and Dove⁷ also agree reasonably well with the present result but have steeper temperature dependence. The present results are in excellent agreement with the values calculated by Joseph *et al.*¹⁰

The rate coefficient data for reaction 14 were used to compute values of the rate coefficient for the reverse reaction. Equilibrium constant values were determined at each experimental temperature by using a polynomial fit to the JANAF¹⁷ data (1300 K < T < 1900 K):

$$K_{eq}(T) = 0.125 - (1.39 \times 10^{-4} T) + (7.68 \times 10^{-8} T^2) - (1.42 \times 10^{-11} T^3)$$

The results are presented in Figure 5 together with the results of Roth and Just,⁴ Rabinowitz *et al.*,⁶ Schatz *et al.*,⁸ Clark and Dove,⁷ Joseph *et al.*,¹⁰ and Allara and Shaw.¹³ Our $k_{-14}(T)$ results are described by Arrhenius expression (1308-1825

K):

$$k_{-14}(T) = 3.1 \times 10^{14} \exp(-7600 \text{ K}/T) \text{ cm}^3 \text{ mol}^{-1} \text{ s}^{-1}$$

The extinction coefficient of CH_3 (ϵ_{CH_3}) can be calculated from I_{max} and the known k_{14} , because the value of I_{max} mainly depends on k_{14} and ϵ_{CH_3} . For the temperature range from 1308 K to 1825 K, our value of ϵ_{CH_3} is $5.2 \times 10^5 \text{ cm}^2/\text{mol}$. Our results are close to those of Hwang *et al.*²¹ and Yang *et al.*,²⁵ who conducted experiments with the same Zn lamp and do not show any, or at most a very weak, dependence on temperature.

Acknowledgment. This research was supported by KOSEF (941-0300-016-2), the Basic Science Research Institute, Ministry of Education, Korea (BSRI-94-3419), the Gas Research Institute and the Robert A. Welch Foundation.

References

1. Fenimore, C. P.; Jones, G. W. *J. Phys. Chem.* **1961**, *65*, 200.
2. Peeters, J.; Mahnen, G. *14th Symposium (International) on Combustion*; The Combustion Institute, Pittsburgh, 1973; p 133.
3. Biordi, J. C.; Lazzara, C. P.; Papp, J. F. *Combust. Flame* **1976**, *26*, 57.
4. Roth, P.; Just, Th. *Ber. Bunsen-Ges. Phys. Chem.* **1975**, *79*, 682.
5. Möller, W.; Mozzhukhin, E.; Wagner, H. Gg. *Ber. Bunsen-Ges. Phys. Chem.* **1986**, *90*, 854.
6. Rabinowitz, M. J.; Sutherland, J. W.; Patterson, P. M.; Klemm, R. B. *J. Phys. Chem.* **1991**, *95*, 674.
7. Clark, T. C.; Dove, J. E. *Can. J. Chem.* **1973**, *51*, 2147.
8. Schatz, G. C.; Wagner, A. F.; Dunning, T. H. *J. Phys. Chem.* **1984**, *88*, 221.
9. Steckler, R.; Dykema, K. J.; Brown, F. B.; Hancock, G. C.; Truhlar, D. G. *J. Phys. Chem.* **1987**, *87*, 7024.
10. Joseph, T.; Steckler, R.; Truhlar, D. G. *J. Phys. Chem.* **1987**, *87*, 7036.
11. Warnatz, J. In *Combustion chemistry*; Gardiner, Jr. W. C., Ed.; Springer-Verlag: New York, 1984.
12. Shaw, R. J. *J. Phys. Chem. Ref. Data* **1978**, *7*, 1179.
13. Allara, D. L.; Shaw, R. J. *J. Phys. Chem. Ref. Data* **1980**, *9*, 523.
14. Tsang, W.; Hampson, R. F. *J. Phys. Chem. Ref. Data* **1986**, *15*, 1087.
15. Hardy, J. E.; Ph.D. Thesis, The University of Texas, Austin **1976**.
16. Gardiner, Jr. W. C.; Walker, B. F.; Wakefield, C. B. In *Shock waves in chemistry*; Lifshitz, A., Ed.; Marcel Dekker, New York, 1981; p 319.
17. Stull, D. R.; Prophet, H. *JANAF Thermochemical tables*; 2nd Ed., US GPO, Washington, 1971; NSRDS-NBS, Circular No. 37.
18. Gordon, S.; McBride, B. J. *Computer program for calculation of complex chemical equilibrium compositions, rocket performance, incident and reflected shock waves, and Chapman-Jouguet Detonations*; NASA SP-273, NASA, Washington, March **1976**.
19. Renaud, R.; Leitch, L. *Can. J. Chem.* **1954**, *32*, 545.
20. Gardiner, Jr. W. C.; Hwang, S. M.; Rabinowitz, M. J. *Energy and Fuels* **1987**, *1*, 545.
21. Hwang, S. M.; Rabinowitz, M. J.; Gardiner, Jr. W. C. *Chem. Phys. Letters* **1993**, *205*, 157.
22. Davidson, D. F.; Chang, A. Y.; Di Rosa, M. D.; Hanson, R. K. *J. Quant. Spectrosc. Radiat. Transfer* **1993**, *49*, 559.
23. Gardiner, Jr. W. C. *J. Phys. Chem.* **1977**, *81*, 2367.
24. Hindmarsh, A. C. *Lawrence Livermore Solver for Ordinary Differential Equations* Version of Sept. 23, **1980**.
25. Yang, H.; Lissianski, V.; Okoroanyanwu, J. U.; Gardiner, Jr. W. C.; Shin, K. S. *J. Phys. Chem.* **1993**, *97*, 10042.